Vol 11 No 1, January 2002
1009-1963/2002/11(01)/0066-06

Chinese Physics

© 2002 Chin. Phys. Soc.
and IOP Publishing Ltd

Magnetization reversal mechanism of magnetic tunnel junctions*

Liu Cun-Ye(刘存业)[a)b)], Li Jian(李 建)[a)], Wang Yue(王 跃)[a)],
Chen Jian-Yong(陈建勇)[a)], Xu Qing-Yu(徐庆宇)[b)], Ni Gang(倪 刚)[b)],
Sang Hai(桑 海)[b)], and Du You-Wei(都有为)[b)]

[a)] *Department of Physics, Southwest China Normal University, Chongqing* 400715, *China*

[b)] *State Key Laboratory of Solid State Microstructures, Nanjing University, Nanjing* 210093, *China*

(Received 2 April 2001; revised manuscript received 22 August 2001)

Using the ion-beam-sputtering technique, we have fabricated $Fe/Al_2O_3/Fe$ magnetic tunnelling junctions (MTJs). We have observed double-peaked shapes of curves, which have a level summit and a symmetrical feature, showing the magnetoresistance of the junction as a function of applied field. We have measured the tunnel conductance of MTJs which have insulating layers of different thicknesses. We have studied the dependence of the magnetoresistance of MTJs on tunnel conductance. The microstructures of hard- and soft-magnetic layers and interfaces of ferromagnets and insulators were probed. Analysing the influence of MJT microstructures, including those having clusters or/and granules in magnetic and non-magnetic films, a magnetization reversal mechanism (MRM) is proposed, which suggests that the MRM of tunnelling junctions may be explained by using a group-by-group reversal model of magnetic moments of the mesoscopical particles. We discuss the influence of MTJ microstructures, including those with clusters or/and granules in the ferromagnetic and non-magnetic films, on the MRM.

Keywords: tunnelling junction, magnetoresistance, spin-dependent scattering
PACC: 7340G, 7220M

1. Introduction

Magnetic multi-layer films constitute a new type of nanostructure which has aroused keen interest because of their unusual magnetic and transport properties. They are obtained by alternately depositing layers of ferromagnetic and non-magnetic elements on a substrate. Ferromagnetic tunnel junctions, tunnelling between ferromagnet–insulator–ferromagnet (FM–I–FM) trilayer planar junctions, are one type of magnetic multi-layer film. The magnetoresistance (MR) of ferromagnetic tunnel junctions made of alternating layers of magnetic metal and insulators has recently aroused much interest due to its potential applications as magnetic sensors and high density memories.[1,2] For these two applications, it is crucial to lower the junction resistance to values near or below a few $k\Omega \times \mu m^2$, such that the submicrometre devices have switching times in the nanosecond range, or present competitive signal-to-noise ratios.[3]

At room temperature, giant magnetoresistance effect (GMR) of the magnetic tunnel junction (MTJ) relates to the fact that quantum tunnelling of electrons between two ferromagnetic electrodes separated by a thin insulator is a spin-dependent phenomenon. The tunnelling probability of electrons and the MR of a tunnel junction are controlled by the relative orientation of the magnetization in its ferromagnetic electrodes. Therefore, this requires a pair of electrodes of which the orientation of each magnetization can be reversed independently. Usually, a magnetically hard–soft system is used for this purpose. In the hard–soft magnetic system, the magnetic moments of the two ferromagnetic layers are formed from magnetic materials with different magnetic switching fields. The magnetic moments of the two layers can then be arranged to be parallel or anti-parallel in certain magnetic field ranges.

Junctions with large room temperature tunnelling magnetoresistance (TMR) use Al_2O_3 as an insulating barrier, which is prepared by deposition of a thin Al layer followed by plasma oxidization or natural oxidizing in air.[4–6] To create an Al_2O_3 barrier, one can also deposit the tunnel barrier directly by using the bulk compound as a starting material; however, the yield

*Project supported by the State Key Program of Basic Research of China(Grant No. G1999064508), and the National Natural Science Foundation of China (Grant No. 19890310{4}).

and reproducibility are less. Obtaining good uniformity and optimal metal layer thickness depends significantly on the surface roughness of the bottom film electrode and the substrate temperature, as well as on other parameters such as deposition method, rate, and the nature of the material, etc. As will be shown in this paper, we have fabricated $Fe/Al_2O_3/Fe$ magnetic tunnel junctions (MTJs), in which the bottom layer was deposited on the Si substrate as the hard-magnetic electrode and the top layer was deposited on the alumina film as the soft-magnetic electrode, using the ion-beam-sputtering method. Our study deals with the microstructure of the $Fe/Al_2O_3/Fe$ MTJs with relation to the TMR effect.

2. Experimental details

The $Fe/Al_2O_3/Fe$ MTJ samples were prepared on (111)Si substrates using the ion-beam-sputtering technique.[5] The high vacuum system is equipped with a Kauffman ion gun. After being ionized in the high-voltage chamber, the argon ion beam with the energy of 1.2keV bombarded the target at the incident angle of 45°. To obtain homogeneous film samples, the single-crystal silicon substrates were installed at the direction of the reflection angle where the maximum deposition ratio is achieved, and the sputtered specimens were deposited on them. The distances from the target to both the ion gun and substrate support were 15 cm. The targets were made of pure Fe or Al. The FM–I–FM devices were patterned by using metal shadow masks and were prepared in a high vacuum system with a base pressure of 2.7×10^{-4}Pa. The films were deposited in an atmosphere of 2.7×10^{-2}Pa argon. The bottom Fe layers were deposited at a substrate temperature T_s=250°C, and the top Fe layers were deposited at a substrate temperature T_s=24°C. After depositing the bottom Fe layers, the aluminium film was deposited at room temperature, covering the entire bottom layer to form the insulating tunnel barrier. The deposited aluminium film was then exposed to air for about 72h to create an insulating layer of Al_2O_3.

The microstructures of the FM–I–FM devices were analysed by X-ray photoelectron spectroscopy (XPS), atomic force microscopy (AFM) and high-resolution electron microscopy (HREM). The bottom Fe layers are well crystallized, because of the effect of the (111) Si substrate, and the top Fe layers are in an amorphous state. The dependence of the concentrations of Al, O and Fe elements on the depth of the sample is shown in Fig.1. The difference in the microstructures of the two Fe layers leads to different magnetic properties.

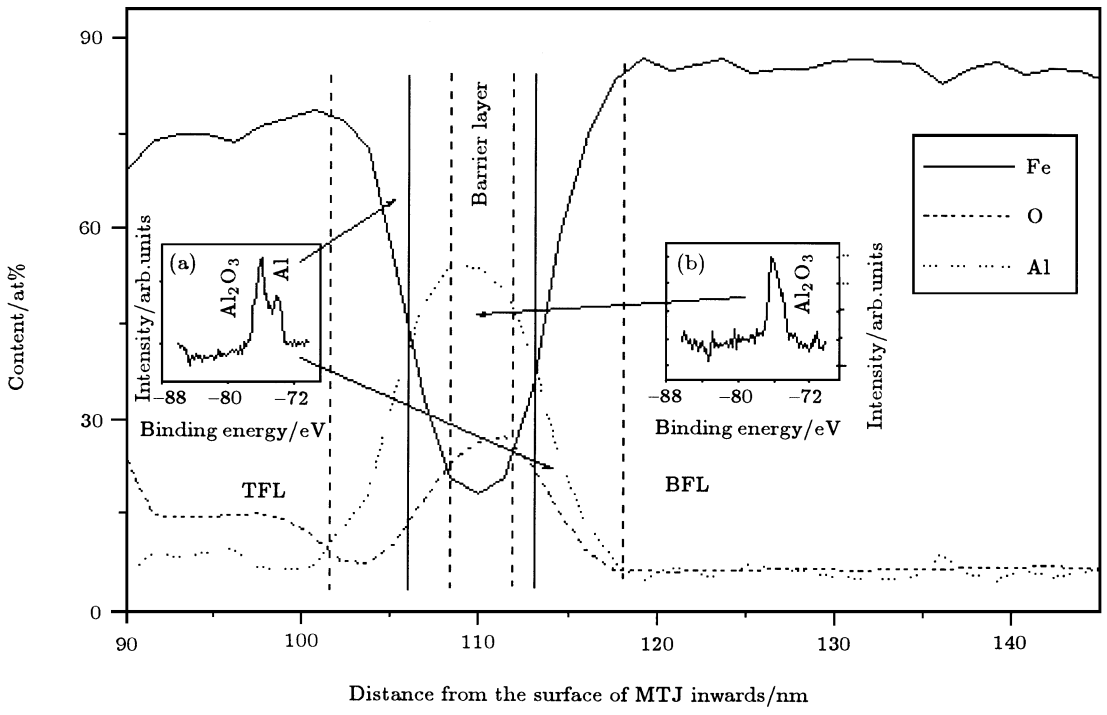


Fig.1. The depth dependence of compositions and microstructures of the sample.

The change in MR of the FM–I–FM devices was measured in an applied magnetic field up to 16000A/m at room temperature. To prove that tunnelling is the main source of conductance, $I(V)$ characteristics were taken for several junctions. The I–V curves, taken from 0 to 0.5V, also confirm the quality of the junctions. The MR value was calculated according to $\Delta R/R = (R_{\uparrow\downarrow} - R_{\uparrow\uparrow})/R_{\uparrow\uparrow}$ and a change in MR of 5.89% was observed. $R_{\uparrow\downarrow}$ and $R_{\uparrow\uparrow}$ are the resistance with magnetization of the two ferromagnetic layers, anti-parallel or parallel.

3. Results and discussion

Many limiting factors can reduce the MR effect: orange peel coupling between ferromagnetic films due to surface roughness,[7] interfacial and barrier spin scattering, ferromagnetic surface degradation, domain walls, etc. Therefore, in the tunnel junction there should be a barrier that is uniform, free from pinholes and thin enough to allow electron tunnelling, together with good metal surfaces.

The quantum model of the GMR developed by Levy *et al.*[8,9] has introduced spin-dependent scattering potentials for both interface and bulk scattering. To understand the microscopic origin of the TMRs, it is important to know which are scattering centres responsible for the TMR effect and where they are located. Several groups have been carrying out research on this.[10−13] This research shows that the high MR value in magnetic multi-layer films is mainly due to spin scattering effects occurring at the interfaces. In magnetic multi-layer films where the contribution of interfacial scattering to the GMR has been suppressed, by increasing the thickness of the ferromagnetic layer, evidence has been found of the presence of a small but not negligible contribution from the spin-dependent scattering within the bulk of the magnetic layer.

As interfacial scattering is important for the GMR effect, the roughness of the interface has great importance. It is difficult to have a complete understanding of the interfacial microstructure because of its strong dependence on growth conditions. The bottom Fe layers and substrate in-plane have lattice constants of 0.28864 and 0.54282nm, respectively. The Fe films grow on the substrate from grain to grain, and a large lattice mismatch strain may be experienced by the films. It is important to realize that the lattice constants of a free-standing Fe film may differ appreciably from the bulk lattice constant of Fe. Due to the random columnar arrangement of the grains along the layer, the roughness of the as-sputtered Fe layer is influenced by the shape, size and distribution of grains. So it is not surprising that the Al_2O_3/Fe interface waves irregularly after depositing a thin layer of alumina. The section images of the as-sputtered Fe layer, aluminium and aluminium oxide layers were observed using nanoscope AFM, as depicted in Fig.2. The surface roughness was estimated from the corresponding images. The surface roughness of the bottom Fe layer and the alumina barrier are about 0.231 and 0.763nm, respectively. The rough interface is a factor that decreases the TMR.

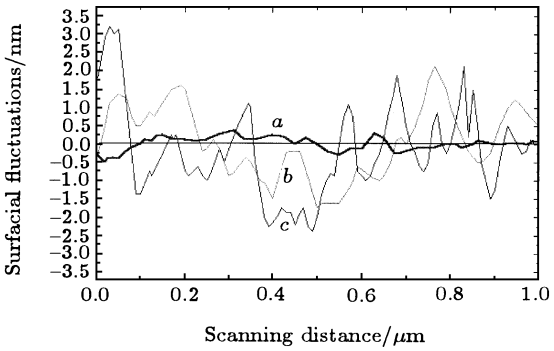


Fig.2. The distance dependence of the surface fluctuations of the bottom Fe layer and the barrier. Labels *a*, *b* and *c* correspond to the bottom Fe layer, aluminium and aluminium oxide barrier, respectively.

An examination of the cross-section image shows that the top Fe layers, seen as the region of light contrast, correspond to a fractal growth appearance of Fe clusters. The strong dark contrast of the bottom Fe layers corresponds to the compact growth regions where Fe crystallites are oriented close to the diffracting conditions.[15] The barrier itself, which is readily identified as the central region of lighter contrast, shows a random appearance corresponding to the alumina amorphous state. Because of the large film thickness and reduced surface anisotropy of the top Fe layers, the magnetization is predicted to be uniform in the plane. Small Fe clusters in this are identified as vortex phases or single-domain phases. Their magnetization reversal proceeds by group jumping under the action of fields. The magnetic structure mutation of the top Fe layer is sketched in Fig.3. In Fig.4, the magnetization curves of the top Fe layers shows a parallelogram loop, with a coercive field window from about 4000 to 5600A/m. This is the first operating field window of the sample. Therefore, under positive

or reversed applied fields above 6000A/m, the magnetization reversal of the top Fe layer is completed and it can be considered as being in a single-domain state. Consequently, the magnetic state of the top Fe layer influences the amplitude and the shape of the upward part of the TMR signal.

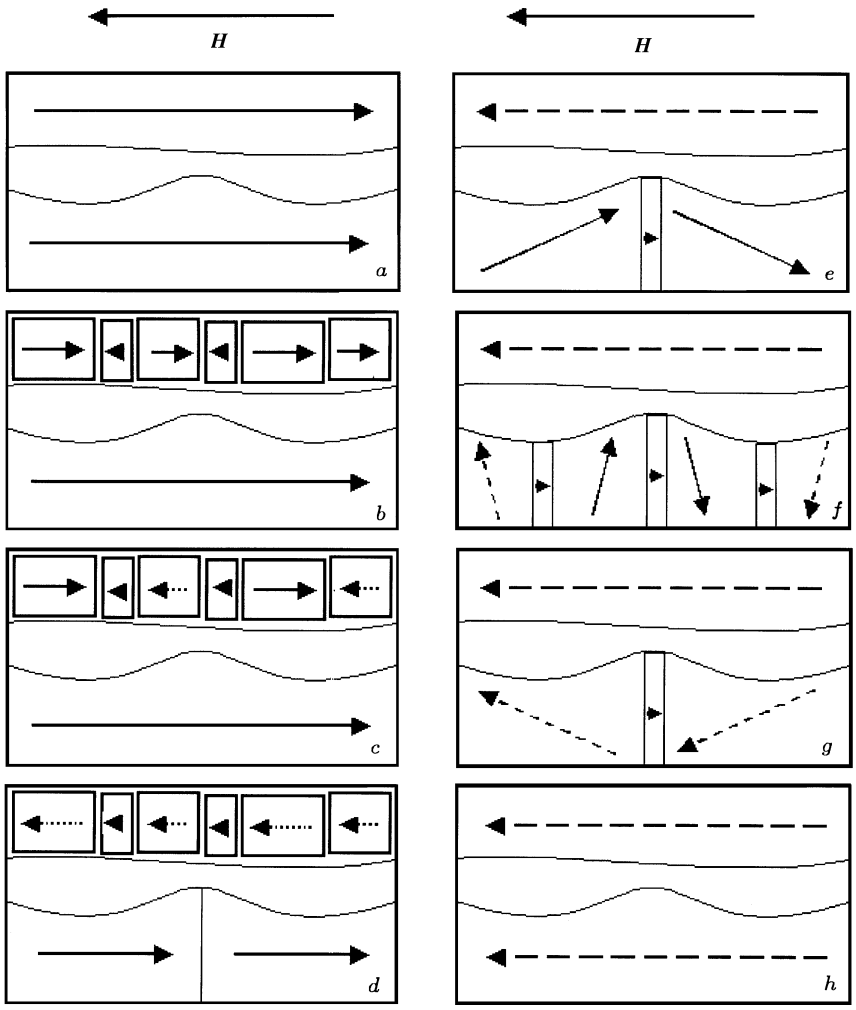


Fig.3. Schematic diagram of the micromagnetic configurations and magnetization reversals for barrier adjacent magnetic layers. The middle layers are tunnelling barriers. Labels from a to h refer to the corresponding TMR curves in Fig.4.

For the bottom Fe layer, we assume that the model for magnetization reversal may be based on the well-known ripple domain configuration in thin magnetic films.[15−18] The Fe magnetic layer is polycrystalline and made of small magnetic grains coupled by exchange interactions. On the microscopic scale, an effective local anisotropy can be defined in terms of an effective correlation. This correlation is sensitive to the spatial variation of the anisotropy, to the magnetic moment and the coupling strength between grains, and to thermal fluctuations. The coupling strength depends on the thickness of the magnetic film.[17] The domain structures with Néel-type walls in the bottom Fe layers are shown in the lower part of each frame of Fig.3. A characteristic ripple structure starts to appear when either the thickness or the coupling between grains is increased.

On the plateau of Fig.4, the magnetization of both electrodes are strongly anti-ferromagnetically coupled and each layer is uniformly magnetized. The TMR curves in Fig.4 were plotted according to $\mathrm{TMR}(H)=100\times[R(H)-R_{\uparrow\downarrow}]/R_{\uparrow\uparrow}$, where $R(H)$ is the junction resistance as a function of the applied field. The width of the plateau was decided by operating field windows of the top and bottom Fe layer electrodes. When the external field is reduced from satu-

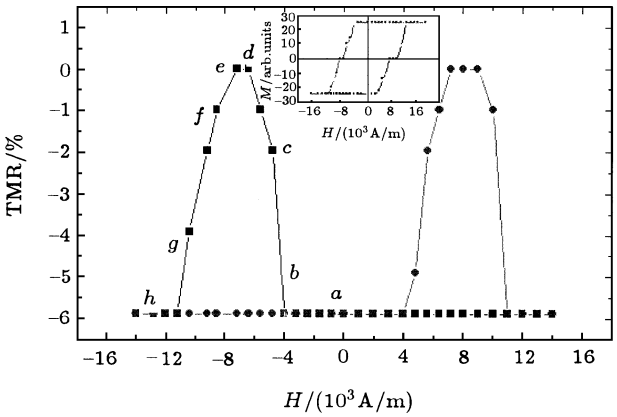


Fig.4. Measured TMR effect of the sample. Labels $a-h$ on the curve refer to the corresponding magnetic configurations in Fig.3. The inset shows the magnetization curves corresponding to the TMR signal.

ration to zero and then reversed, the magnetized state of the bottom Fe layer electrode remains stable until the field is close to the end of the plateau. The bottom Fe layer electrode acts as a rigid block only for applied fields usually less than about 7600A/m, which is less than the secondary operating field window of 8000–9600A/m. By increasing the field in the reversed direction, a domain structure begins to form corresponding to magnetic charge accumulations. The moments inside the uniformly magnetized regions weakly coupled with the neighbouring regions will start to rotate. Then regions with a different sense of rotation of their local magnetization meet, and correlated Néel walls start to establish. As the field further increases, the neighbouring moments are dragged in the field direction by exchange interactions and the effective length of the 360° Néel walls is increased. The walls remain pinned at fields higher than the field for which the reversal of the magnetization in domains is almost completed (see Fig.4). This unstable situation is overcome at a field of about ±9600A/m, which is large enough to allow the walls to escape from the pinning centres. The distribution of the depinning fields is consistent with the gradual disappearance of the 360° walls. After the reversal is complete, for field larger than the local pinning fields, the walls disappear. The process of magnetization reversal of the bottom Fe layer electrode, from the creation of the domain structure to the complete disappearance of the Néel walls, affect the shape of the upper part of the TMR signal. The reversal process of the MTJ is sketched in Fig.4.

4. Summary

In a MTJ device, the spin-dependent transport properties of electrons are strongly dependent on the magnetic state of the pair of electrodes and the two magnetic metal–oxide interfaces. The resistance of the junction depends on the relative orientation of the magnetization of the magnetic layers. When the domain structures of the magnetic layers are changed, the resistance of the junction is strongly influenced. The two operating field windows of electrodes are characteristic of the MTJ. The plateaus of the TMR curves occur between these two windows. The shape of the TMR curves is strongly dependent on the microscopic magnetic characteristic of electrodes. The tunnelling current will decrease due to the increasing distance through the barrier. Therefore, the preferential conduction channels are the shortest paths for electrons to travel across the barrier. The relative orientation of the ferromagnetic moments directly across the barrier is the most important factor determining the magnitude of the tunnelling current. The TMR signal depends on the local magnetic configuration of magnetic layers directly at the interface with the tunnel barrier. The domains and walls give rise to conduction channels with different resistance decided by the lateral fluctuation of the angle between the magnetic moments of layers in contact with the tunnel barrier. In other words, Néel walls, having the magnetization in their centre opposite to the magnetization of the domain, strongly influence the amplitude and shape of the TMR signal. The junction resistance corresponds to all sections of the junction containing a magnetic domain or a domain wall with a given local orientation relative to the bilayer direction. At the interface with the tunnel barrier, the magnetic fluctuations depend on micro-magnetic defects, domains, and the domain walls of the electrode. These fluctuations, which modulate the resistance of the tunnel junction, strongly affect the shape and the amplitude of the TMR curve.

Acknowledgment

One of the authors (H Sang) would like to thank the Keli Foundation.

References

[1] Miyazaki T and Tezuka N 1995 *J. Magn. Magn. Mater.* **139** 1231

[2] Moodera J S, Kinder L R, Wong T M and Meservey R 1995 *Phys. Rev. Lett.* **74** 3273

[3] Daughton J M 1997 *J. Appl. Phys.* **81** 3758

[4] Schad R, Allen D, Zangari G, Zana I, Yang D, Tondra M and Wang D 2000 *Appl. Phys. Lett.* **76** 607

[5] Chen H, Xu Q Y, Ni G, Lu J, Sang H, Zhang S Y and Du Y W 1999 *J. Appl. Phys.* **85** 5798

[6] Sun J J, Shimazawa K, Kasahara N, Saruki S, Kagami T, Redon O, Araki S, Morita H and Matsuzaki M 2000 *Appl. Phys. Lett.* **76** 2424

[7] Moodera J S and Kinder L R 1996 *J. Appl. Phys.* **79** 4724

[8] Lery P M, Zhang S and Fert A 1990 *Phys. Rev. Lett.* **65** 1643

[9] Zhang S, Lery P M and Fert A 1992 *Phys. Rev.* B **45** 8689

[10] Sharma M, Wang S X and Nickel J H 1999 *Phys. Rev. Lett.* **82** 616

[11] Parkin S S P 1993 *Phys. Rev. Lett.* **71** 1641

[12] Pommier J, Meyer P, Penissard G and Ferre J 1990 *Phys. Rev. Lett.* **65** 2054

[13] Kashuba A B and Pokrovsky V L 1993 *Phys. Rev.* B **48** 5355

[14] Wang D M and Wu Z Q 2000 *Chin. Phys.* **9** 369

[15] Laver K D 1968 *Thin Solid Films* **2** 149

[16] Herzer H 1989 *IEEE Trans. Magn.* **25** 3327

[17] Berkov D V and Gorn N L 1998 *Phys. Rev.* B **57** 14332

[18] Tiusan C, Dimopoulos T, Ounadjela K, Hehn M and Henry Y 2000 *Phys. Rev.* B **61** 580